HHS Public Access

Author manuscript

Heart Rhythm. Author manuscript; available in PMC 2016 April 01.

Published in final edited form as:

Heart Rhythm. 2015 April ; 12(4): 668–672. doi:10.1016/j.hrthm.2014.12.021.

Comparison of Pre-Existing Versus Ablation-Induced Late Gadolinium Enhancement on Left Atrial Magnetic Resonance Imaging

Kotaro Fukumoto, MD, PhD[*], **Mohammadali Habibi, MD**[*], **Esra Gucuk Ipek, MD**[*], **Irfan M. Khurram, MD**[*], **Stefan L. Zimmerman, MD**[†], **Vadim Zipunnikov, PhD**[‡], **David D. Spragg, MD**[*], **Hiroshi Ashikaga, MD, PhD**[*], **John Rickard, MD**[*], **Joseph E. Marine, MD, FHRS**[*], **Ronald D. Berger, MD, PhD, FHRS**[*], **Hugh Calkins, MD, FHRS**[*], and **Saman Nazarian, MD, PhD, FHRS**[*,§]

[*] Division of Cardiology, Johns Hopkins University, Baltimore, MD

[†] Department of Radiology, Johns Hopkins University, Baltimore, MD

[‡] Department of Biostatistics, Johns Hopkins University, Baltimore, MD

[§] Department of Epidemiology, Johns Hopkins University, Baltimore, MD

Abstract

Background—Post-ablation atrial fibrillation (AF) recurrence is positively associated with the extent of pre-existing left atrial (LA) late gadolinium enhancement (LGE) on magnetic resonance imaging (MRI), but negatively associated with the extent of post-ablation LGE regardless of proximity to the pulmonary vein antra. The characteristics of pre- versus post-ablation LA LGE may provide insight into this seeming paradox and inform future strategies for ablation.

Objective—To define the characteristics of pre-existing versus ablation-induced LA LGE

Methods—LGE-MRI was prospectively performed before and ≥3 months after initial ablation in 20 patients. The intra-cardiac locations of ablation points were co-registered with the corresponding sites on axial planes of post-ablation LGE-MRI. The image intensity ratio (IIR), defined as LA myocardial MRI signal intensity divided by the mean LA blood pool intensity, and LA myocardial wall thickness, were calculated on pre- and post-ablation images.

Results—Imaging data from 409 pairs of pre- and post-ablation axial LGE-MRI planes and 6961 pairs of pre- and post-ablation image sectors were analyzed. Ablation-induced LGE revealed higher IIR, suggesting greater contrast uptake and denser fibrosis compared to pre-existing LGE

Corresponding author: Saman Nazarian, MD, PhD, Johns Hopkins University Carnegie 592A, 600 N. Wolfe Street, Baltimore, MD 21287 Phone: 410-614-2751, Fax: 410-502-4854 snazarian@jhmi.edu.

Disclosures: Dr. Nazarian is a scientific advisor to Biosense-Webster Inc and Medtronic Inc, and principal investigator for research funding to Johns Hopkins University from Biosense-Webster Inc.

(IIR 1.25±0.25 vs. 1.14±0.15, p<0.001). Additionally, ablation-induced LGE regions had thinner LA myocardium (2.10±0.67 vs. 2.37±0.74 mm, P<0.001).

Conclusions—Regions with ablation-induced LGE exhibit increased contrast uptake, likely signifying higher scar density, and thinner myocardium compared to regions with pre-existing LGE. Future studies to examine the association of post ablation LGE intensity and non-uniformity with ablation success may inform strategies to optimize ablation outcome.

Keywords

Atrial fibrillation; MRI; late gadolinium enhancement; fibrosis; catheter ablation

Introduction

Radiofrequency catheter ablation is increasingly used for treatment of drug refractory atrial fibrillation (AF).[1] The presence of AF is associated with left atrial (LA) scar,[2-7] which is detectable by late gadolinium enhancement (LGE) cardiac magnetic resonance imaging (MRI).[8, 9] We recently described the image intensity ratio (IIR), calculated by normalization of the LA myocardial pixel intensity by the blood pool intensity, and validated quantitative IIR thresholds of >0.97 and >1.61 corresponding to local bipolar voltage thresholds of <0.5 and <0.1 mV, respectively.[10] Prior studies have reported a positive association between the extent of pre-existing LA LGE and AF recurrence following ablation.[8, 11-13] Paradoxically, however, the extent of post-ablation LGE has been described to have a negative association with AF recurrence regardless of proximity to the pulmonary vein antra.[14-16] A recent study demonstrated differences in the extent and distribution of pre- and post-ablation LA LGE.[17] We hypothesized that differences in the homogeneity of LGE versus non-enhanced myocardium, i.e. the density of pre-existing versus ablation-induced scar, mediate the disparate association of each LGE type with arrhythmia occurrence. Additionally, regions with homogeneous scar are likely to be thinner than regions with scar and intervening surviving myocardium. Therefore, in this study we sought to examine LGE-MRI LA myocardial signal intensity and myocardial thickness differences between pre-existing and ablation-induced LA LGE.

Methods

Study population

Between April 2010 and April 2013, 22 patients were prospectively enrolled to undergo cardiac MRI scans both before and at least three months after their initial radiofrequency catheter ablation for AF. The Johns Hopkins Institutional Review Board approved the study protocol. Written informed consent was obtained from each patient prior to the pre-procedural MRI. Two of 22 patients were excluded due to insufficient imaging data, and the remaining 20 formed the study cohort.

Magnetic Resonance Imaging

MRI acquisition was performed using a 1.5-Tesla MRI scanner (Avanto, Siemens, Erlangen, Germany). LGE-MRI scans were acquired within a range of 10-32 (mean 17±5) minutes

following 0.2 mmol/kg gadolinium injection (gadopentetate dimeglumine; Bayer Healthcare Pharmaceuticals, Montville, NJ) using a fat-saturated three dimensional IR-prepared fast spoiled gradient recalled echo sequence with respiratory navigation and ECG-gating, echo time of 1.52 ms, repetition time of 3.8 ms, in-plane resolution of 1.3 × 1.3, slice thickness of 2.0 mm, and flip angle of 10 degrees. Trigger time for 3D LGE-MRI images was optimized to acquire imaging data during diastole of LA as dictated by inspection of the cine images. The optimal inversion time (TI) was identified with a TI scout scan (median 270 ms, range 240-290 ms) to maximize nulling of LA myocardium. A parallel imaging technique, Generalized Auto-calibrating Partially Parallel Acquisition (GRAPPA, reduction factor 2), was used. Patients with persistent AF were started on antiarrhythmic medication and referred for cardioversion 3-4 weeks prior to MRI and AF ablation. Of all patients, 6 were in AF at the time of baseline imaging and 5 were in AF during follow up.

Image analysis of pre- and post-ablation MRI

QMass MR software (version 7.2, Leiden University Medical Center, Leiden, The Netherlands) was used to quantify LGE extent on pre and post ablation LGE-MRI by an observer that was masked to electroanatomic map (EAM) results. Epicardial and endocardial contours were manually drawn around the LA myocardium on multiplanar reformatted (MPR) axial images (3.5-mm slice thickness), which were reconstructed from axial image data (Figure 1). The anatomical reference point was set at the LA posteroseptum, and the LA myocardium in each axial plane was divided into 20 sectors. The average wall thickness of each sector was calculated. The IIR for each sector, defined as the mean pixel intensity of each sector divided by the mean pixel intensity of the entire LA blood pool, was calculated. Sectors with IIR>0.97 and >1.61 were labeled as LGE and dense LGE, respectively.[10] The pulmonary vein-atrial junction and the mitral annulus were excluded from myocardial contours (Figure 1). To measure inter- and intra-observer variability, the epicardial and endocardial contouring of the entire LA was repeated for a random sample of 5 patients by a second independent observer and by the primary observer, respectively.

Electroanatomical mapping and Radiofrequency catheter ablation

Radiofrequency catheter ablation using the pulmonary vein isolation (PVI) strategy was performed with an EAM system (CARTO3, Biosense Webster, Diamond Bar, CA) and a mapping/ablation catheter with a 3.5-mm open-irrigation tip (Navistar Thermocool, Biosense Webster) in all cases. The position coordinates of all radiofrequency application sites were recorded using the EAM system. Acute PVI was achieved in all subjects. In persistent AF cases, additional ablation was performed including linear roof and floor lines. Patients were observed for 24 hours following the procedure. No immediate postoperative complications were noted.

Co-registration of electroanatomical mapping data and post-ablation MRI

By using previously validated custom software (Volley, Johns Hopkins University, Baltimore, MD),[10, 18] the coordinates of ablation points on EAM were registered to the post-ablation LGE-MRI axial image planes. An observer, masked to IIR results, performed the registration utilizing the pulmonary veno-atrial junctions, the inferior mitral valve, and the

anterior base of the left atrial appendage as anatomical references. Image sectors that corresponded to ablation points from EAM were defined as ablated sectors (Figure 2).

Statistical analysis

Continuous variables are expressed as mean ± standard deviation (SD) and categorical data as numbers or percentages. The IIR and thickness measurements from ablation-induced LGE were compared to IIR and thickness measurements from pre-existing LGE using the non-parametric Wilcoxon-Mann-Whitney test. The multivariable association of LGE type (ablation versus pre-existing) as dependent variable with IIR and thickness as independent variables was also assessed using a binary logit generalized estimating equations model, clustered by patient, and with an exchangeable correlation matrix. The intra-class correlation coefficients for interobserver variability in measuring the IIR were calculated using two-way random effects models. Receiver operator curve analysis was performed to examine the diagnostic performance of IIR for discrimination of ablation-induced LGE from pre-existing LGE. Statistical analyses were performed using STATA (version 12, StataCorp, College Station, Texas).

Results

Patient characteristics

Twenty patients (16 males, age 59±8.8 years, 10 paroxysmal, 10 persistent AF) were enrolled in this study. Four individuals had underlying heart disease (1 prior percutaneous coronary stenting for angina, 1 hypertrophic cardiomyopathy, 2 tachycardia-induced cardiomyopathy). Left ventricular ejection fraction was 61±8.6% (range 35 to 75%) and CHA_2DS_2-VASc score was 1.2 ±0.99 (range 0 to 3). The participant characteristics have been summarized in Table 1.

Pre-ablation MRI

Three-dimensional LGE-MRI with minimal artifacts was obtained in all 20 patients. A total of 6961 image sectors from 409 MPR axial image planes were analyzed. Out of 6961 sectors, 3000 (43%) and 57 sectors (0.8%) exhibited pre-existing LGE (IIR>0.97) and pre-existing dense LGE (IIR>1.61), respectively. The IIR and LA wall thickness of pre-existing LGE were 1.14 ±0.15 (range 0.97 to 1.99) and 2.37±0.74 (range 0.42 to 5.84) mm, respectively.

Registration of EAM data to post-ablation MRI

Post-ablation MRI was performed 287±148 days after the initial AF ablation. The procedural coordinates of a total of 8670 ablation points from the EAM system were registered to the post-ablation LGE-MRI. A total of 6691 sectors from 391 MPR post-ablation image planes were analyzed. A total of 1533 ablated image sectors were identified. Out of 1533 ablated sectors, 1132 (74%) and 91 sectors (5.9%) exhibited ablation-induced LGE (IIR>0.97) and ablation-induced dense LGE (IIR>1.61), respectively. Compared to pre-existing LGE sites, ablation-induced LGE sites had a significantly greater IIR (1.25±0.25, range 0.97 to 2.75, $p<0.001$) and thinner LA wall (2.10±0.67 mm, range 0.37 to 4.85 mm, $p<0.001$) (Figure 3). In the multivariable binary logit generalized estimating

equations model, which was clustered by patient, IIR (β = 2.59, P<0.001) and wall thickness (β = -0.78, P<0.001) were independently associated with ablation-induced LGE.

Inter- and intra-observer variability

A total of 1844 image sectors from 5 patients underwent repeat analysis by the same reviewer and subsequently by a second reviewer for the assessment of intra- and inter-observer variability, respectively. The intra-class correlation for intra-observer variability of the IIR measures was 0.987 (95% CI 0.985-0.989) for reliability of observations. The intra-class correlation for intra-observer variability of the thickness measures was 0.929 (95% CI 0.922-0.935) for reliability of observations. The intra-class correlation for inter-observer variability of the IIR measures was 0.976 (95% CI 0.967-0.982) for reliability of observations. The intra-class correlation for inter-observer variability of the thickness measures was 0.773 (95% CI 0.753-0.791) for reliability of observations.

Discussion

To the best of our knowledge, this is the first study to compare the characteristics of pre-existing versus ablation-induced LGE in LA myocardium. The major finding of our study is that ablation-induced LGE exhibits increased contrast uptake, suggesting higher scar density, and thinner myocardium compared to regions with pre-existing LGE.

Previous studies have demonstrated that the extent of pre-ablation LGE in the LA myocardium positively associates with AF recurrence following catheter ablation.[8, 11, 12] In contrast, the extent of post-ablation LGE in the LA myocardium negatively associates with AF recurrence regardless of the LGE proximity to the pulmonary vein antra.[14-16] Studies from our group as well as others have shown that LGE, with its current resolution, is incapable of detecting all ostial PVI lesions and gaps.[19-21] Therefore, it is unlikely that the presence or absence of gaps mediates the disparate association of the extent of pre-existing versus ablation-induced LGE with the outcome of AF ablation. The characteristics of pre-existing versus ablation induced LGE, as a possible mediator of the paradoxical association of each LGE type with outcome has not been previously investigated.

Prior experimental animal studies have demonstrated that by two months following radiofrequency ablation the myocardium undergoes contraction necrosis and exhibits fibrous scar.[22] LGE-MRI is able to depict not only ventricular but also atrial ablation sites as LGE regions.[9, 16, 23] In our study, the normalized signal intensity of ablation-induced LGE was significantly higher than that of pre-existing LGE. This finding indicates that ablation-induced LGE exhibits different contrast kinetics with greater uptake and/or slower washout of contrast, suggesting more severe fibrosis. Thinner wall thickness was also noted in regions with ablation-induced LGE consistent with prior histological reports of contraction necrosis at ablated sites.[22] Although this study demonstrated statistically significant differences in IIR and LA wall thickness between pre-existing LGE and ablation-induced LGE, there was significant overlap between the ranges of these measures for each LGE type (Figure 3). Nevertheless, important associations of LGE intensity and myocardial thickness with ablation were demonstrated in this study. Based upon these results, scar density and non-uniformity may explain the disparate association of pre and post ablation LGE with AF

recurrence in prior studies. Future studies to examine the association of post ablation LGE intensity and non-uniformity with AF recurrence are warranted and may inform strategies to optimize ablation outcome.

Limitations

The patient sample size is relatively small. However, many distinct non-ablated and ablated image sectors per patient were analyzed. Therefore, statistical power was sufficient for testing the study hypothesis. Our results may be limited by a possibility for positional errors when registering EAM ablation points to corresponding sectors on LGE-MRI based on the registration information obtained by the EAM software. The LGE-MRI sequence used in this study provided a 1.3 × 1.3 mm in-plane resolution and was obtained during ventricular diastole/atrial systole, thus minimizing potential negative effects of motion blurring on atrial wall thickness measurements. Nevertheless, atrial wall thickness may be near the limit of image resolution in some cases. Because of volume averaging, the analyzed LA wall sector may have included blood pool or epicardial fat in some cases. Of all MRI examinations, 27% were performed during AF; however, we found no evidence of association between rhythm at the time of imaging and the IIR ($\beta = 0.04$, $P=0.211$). Information regarding the duration of radiofrequency application and contact force at each site was unavailable. Therefore, ablated sectors in the present study may have included sectors with ineffective lesion delivery.

Conclusion

Our study demonstrates that LA ablation-induced LGE is associated with greater contrast affinity and thinner walls when compared to pre-existing LA LGE. These findings support the presence of dense fibrosis in ablated regions and may underlie the paradoxical association of each LGE type with arrhythmia recurrence.

Acknowledgments

Funding Sources: The study was funded by a Biosense-Webster grant and NIH grants K23HL089333 and R01HL116280 to Dr. Nazarian, the Dr. Francis P. Chiaramonte Foundation, and The Norbert and Louise Grunwald Cardiac Arrhythmia Research Fund. The content is solely the responsibility of the authors and does not necessarily represent the official views of the NIH.

Abbreviations List

AF	atrial fibrillation
LA	left atrial
LGE	late gadolinium enhancement
MRI	magnetic resonance imaging
IIR	image intensity ratio
EAM	electroanatomic map
MPR	multiplanar reformatted

PVI	pulmonary vein isolation
SD	standard deviation
IQR	interquartile range
CI	confidence interval

References

1. Calkins H, Kuck KH, Cappato R, et al. 2012 hrs/ehra/ecas expert consensus statement on catheter and surgical ablation of atrial fibrillation: Recommendations for patient selection, procedural techniques, patient management and follow-up, definitions, endpoints, and research trial design: A report of the heart rhythm society (hrs) task force on catheter and surgical ablation of atrial fibrillation. Developed in partnership with the european heart rhythm association (ehra), a registered branch of the european society of cardiology (esc) and the european cardiac arrhythmia society (ecas); and in collaboration with the american college of cardiology (acc), american heart association (aha), the asia pacific heart rhythm society (aphrs), and the society of thoracic surgeons (sts). Endorsed by the governing bodies of the american college of cardiology foundation, the american heart association, the european cardiac arrhythmia society, the european heart rhythm association, the society of thoracic surgeons, the asia pacific heart rhythm society, and the heart rhythm society. Heart rhythm : the official journal of the Heart Rhythm Society. 2012; 9:632–696. e621. [PubMed: 22386883]
2. Corradi D. Atrial fibrillation from the pathologist's perspective. Cardiovascular pathology : the official journal of the Society for Cardiovascular Pathology. 2014; 23:71–84. [PubMed: 24462196]
3. Corradi D, Callegari S, Maestri R, Benussi S, Alfieri O. Structural remodeling in atrial fibrillation. Nat Clin Pract Card. 2008; 5:782–796.
4. Corradi D, Callegari S, Manotti L, et al. Persistent lone atrial fibrillation: Clinicopathologic study of 19 cases. Heart rhythm : the official journal of the Heart Rhythm Society. 2014; 11:1250–1258. [PubMed: 24560692]
5. Frustaci A, Chimenti C, Bellocci F, Morgante E, Russo MA, Maseri A. Histological substrate of atrial biopsies in patients with lone atrial fibrillation. Circulation. 1997; 96:1180–1184. [PubMed: 9286947]
6. Kostin S, Klein G, Szalay Z, Hein S, Bauer EP, Schaper J. Structural correlate of atrial fibrillation in human patients. Cardiovascular research. 2002; 54:361–379. [PubMed: 12062341]
7. Lin CS, Lai LP, Lin JL, Sun YL, Hsu CW, Chen CL, Mao SJ, Huang SK. Increased expression of extracellular matrix proteins in rapid atrial pacing-induced atrial fibrillation. Heart rhythm : the official journal of the Heart Rhythm Society. 2007; 4:938–949. [PubMed: 17599682]
8. Oakes RS, Badger TJ, Kholmovski EG, et al. Detection and quantification of left atrial structural remodeling with delayed-enhancement magnetic resonance imaging in patients with atrial fibrillation. Circulation. 2009; 119:1758–1767. [PubMed: 19307477]
9. Peters DC, Wylie JV, Hauser TH, Kissinger KV, Botnar RM, Essebag V, Josephson ME, Manning WJ. Detection of pulmonary vein and left atrial scar after catheter ablation with three-dimensional navigator-gated delayed enhancement mr imaging: Initial experience. Radiology. 2007; 243:690–695. [PubMed: 17517928]
10. Khurram IM, Beinart R, Zipunnikov V, et al. Magnetic resonance image intensity ratio, a normalized measure to enable interpatient comparability of left atrial fibrosis. Heart rhythm : the official journal of the Heart Rhythm Society. 2014; 11:85–92. [PubMed: 24096166]
11. Mahnkopf C, Badger TJ, Burgon NS, Daccarett M, Haslam TS, Badger CT, McGann CJ, Akoum N, Kholmovski E, Macleod RS, Marrouche NF. Evaluation of the left atrial substrate in patients with lone atrial fibrillation using delayed-enhanced mri: Implications for disease progression and response to catheter ablation. Heart rhythm : the official journal of the Heart Rhythm Society. 2010; 7:1475–1481. [PubMed: 20601148]

12. McGann C, Akoum N, Patel A, et al. Atrial fibrillation ablation outcome is predicted by left atrial remodeling on mri. Circ-Arrhythmia Elec. 2014; 7:23–30.
13. Verma A, Wazni OM, Marrouche NF, et al. Pre-existent left atrial scarring in patients undergoing pulmonary vein antrum isolation: An independent predictor of procedural failure. Journal of the American College of Cardiology. 2005; 45:285–292. [PubMed: 15653029]
14. McGann C, Kholmovski E, Blauer J, et al. Dark regions of no-reflow on late gadolinium enhancement magnetic resonance imaging result in scar formation after atrial fibrillation ablation. Journal of the American College of Cardiology. 2011; 58:177–185. [PubMed: 21718914]
15. McGann CJ, Kholmovski EG, Oakes RS, et al. New magnetic resonance imaging-based method for defining the extent of left atrial wall injury after the ablation of atrial fibrillation. Journal of the American College of Cardiology. 2008; 52:1263–1271. [PubMed: 18926331]
16. Peters DC, Wylie JV, Hauser TH, Nezafat R, Han YC, Woo JJ, Taclas J, Kissinger KV, Goddu B, Josephson ME, Manning WJ. Recurrence of atrial fibrillation correlates with the extent of post-procedural late gadolinium enhancement a pilot study. Jacc-Cardiovasc Imag. 2009; 2:308–316.
17. Malcolme-Lawes LC, Juli C, Karim R, et al. Automated analysis of atrial late gadolinium enhancement imaging that correlates with endocardial voltage and clinical outcomes: A 2-center study. Heart rhythm : the official journal of the Heart Rhythm Society. 2013; 10:1184–1191. [PubMed: 23685170]
18. Sasaki T, Miller CF, Hansford R, et al. Myocardial structural associations with local electrograms a study of postinfarct ventricular tachycardia pathophysiology and magnetic resonance-based noninvasive mapping. Circ-Arrhythmia Elec. 2012; 5:1081–1090.
19. Spragg DD, Khurram I, Zimmerman SL, Yarmohammadi H, Barcelon B, Needleman M, Edwards D, Marine JE, Calkins H, Nazarian S. Initial experience with magnetic resonance imaging of atrial scar and co-registration with electroanatomic voltage mapping during atrial fibrillation: Success and limitations. Heart rhythm : the official journal of the Heart Rhythm Society. 2012; 9:2003–2009. [PubMed: 23000671]
20. Arujuna A, Karim R, Caulfield D, Knowles B, Rhode K, Schaeffter T, Kato B, Rinaldi CA, Cooklin M, Razavi R, O'Neill MD, Gill J. Acute pulmonary vein isolation is achieved by a combination of reversible and irreversible atrial injury after catheter ablation evidence from magnetic resonance imaging. Circ-Arrhythmia Elec. 2012; 5:691–700.
21. Taclas JE, Nezafat R, Wylie JV, Josephson ME, Hsing J, Manning WJ, Peters DC. Relationship between intended sites of rf ablation and post-procedural scar in af patients, using late gadolinium enhancement cardiovascular magnetic resonance. Heart rhythm : the official journal of the Heart Rhythm Society. 2010; 7:489–496. [PubMed: 20122877]
22. Nath S, DiMarco JP, Haines DE. Basic aspects of radiofrequency catheter ablation. Journal of cardiovascular electrophysiology. 1994; 5:863–876. [PubMed: 7874332]
23. Harrison JL, Jensen HK, Peel SA, et al. Cardiac magnetic resonance and electroanatomical mapping of acute and chronic atrial ablation injury: A histological validation study. European heart journal. 2014; 35:1486–1495. [PubMed: 24419806]

Clinical Perspectives

Post-ablation atrial fibrillation recurrence is positively associated with the extent of pre-existing left atrial late gadolinium enhancement, but negatively associated with the extent of post-ablation enhancement on magnetic resonance imaging. We sought to define the characteristics of pre-existing versus ablation-induced left atrial late gadolinium enhancement. Our findings indicate that regions with ablation-induced enhancement exhibit increased contrast uptake, likely signifying higher scar density, and thinner myocardium compared to regions with pre-existing enhancement. These differences among the characteristics of pre- versus post-ablation atrial late gadolinium enhancement provide insight into the paradoxical association of each scar type with outcome and may inform future strategies for ablation.

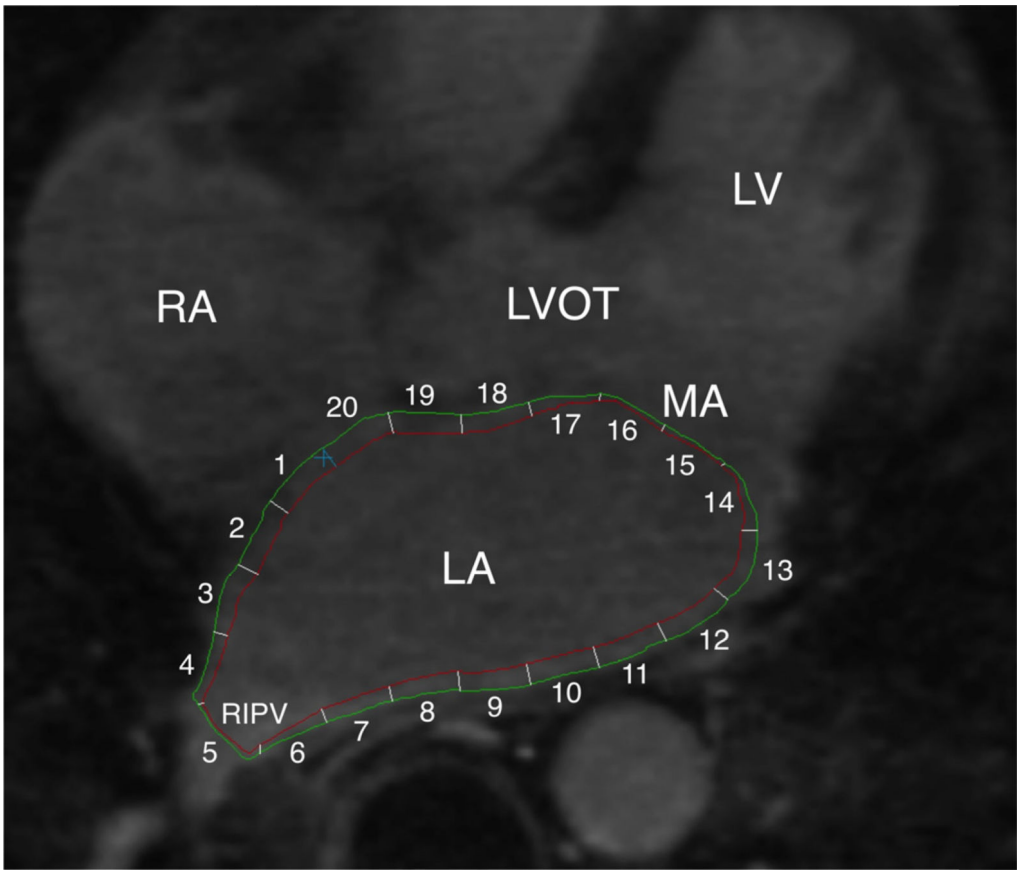

Figure 1. Endocardial and epicardial LA contours on a representative case

The endocardial (red) and epicardial contours (green) were drawn on MPR axial image planes from LGE-MRI. LA myocardium between two contours was divided into 20 sectors and the mean pixel intensity of each sector was calculated. Pulmonary veno-atrial junction (sector 5) and the mitral valve (sectors 14-17) were excluded from analyses. Ao: aorta, LV: left ventricle, RA: right atrium, RIPV: right inferior PV.

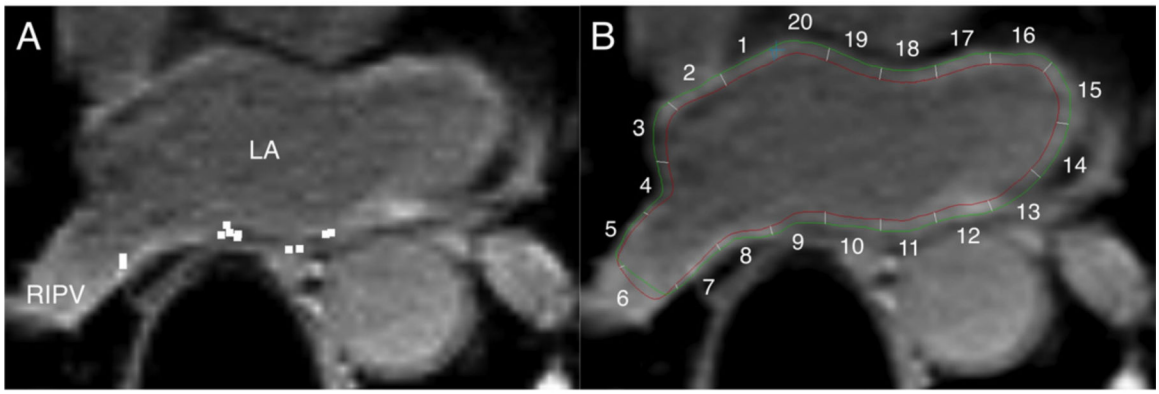

Figure 2. Registration of EAM data to post-ablation LGE-MRI

A: Location data of ablation sites on EAM (white square dots) were registered to the post-ablation MRI by using custom software. B: The LA endocardial and epicardial contours are drawn onto the axial image at the same level as Panel A. LA sectors on axial image planes corresponding to ablated sites were identified. In this example, sectors 7, 9, 10, 11 were identified as ablated sectors.

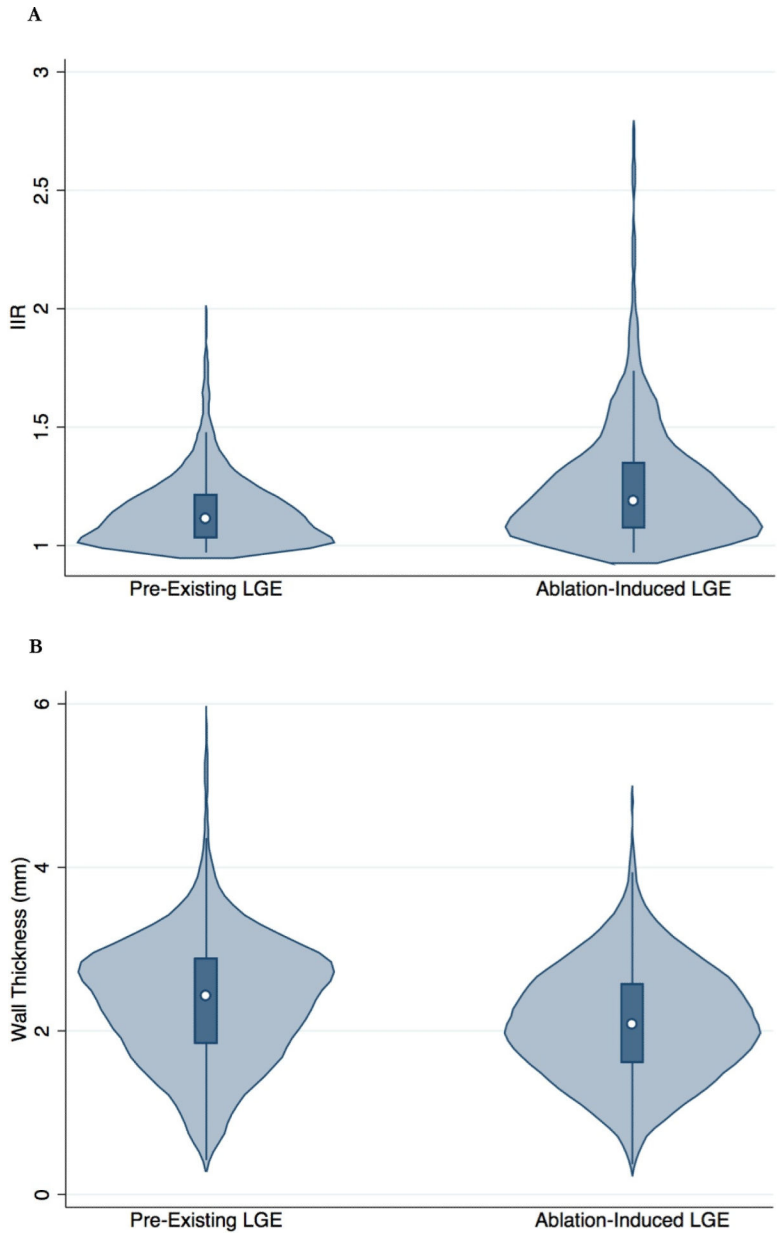

Figure 3. Distribution of IIR and wall thickness in pre-existing and ablation-induced LGE

The violin plots (light blue) show the probability density of IIR (A) and wall thickness (B) for all LA myocardial sectors with pre-existing and ablation-induced LGE. The white dot shows the median value and the dark blue box represents the interquartile range, with the dark blue vertical line extending to the lower and upper adjacent values.

Table 1

Patient characteristics (N = 20)*

Age (years)	59±8.8
Male	16 (80%)
BMI†	29±5.6
Type of AF	
Paroxysmal	10 (50%)
Persistent	10 (50%)
AF duration (years)	6.9±5.7
LVEF‡ (%)	61±8.6
CHA2DS2-VASc	1.2±0.99
Duration from preoperative MRI to ablation (days)	3.3±6.6
Duration from ablation to postoperative MRI (days)	287±148
Ablation protocols	
PVI	20 (100%)
LA roof line ablation	3 (15%)
CFAE§ ablation	1 (5%)
Lateral mitral isthmus linear ablation	0

*Data are presented as mean ± SD or as n (%).

†BMI: body mass index

‡LVEF: left ventricular ejection fraction

§CFAE: complex fractionated atrial electrograms